The Influences of I_h on Temporal Summation in Hippocampal CA1 Pyramidal Neurons: A Modeling Study

Adrien E. Desjardins[1,2], Yue-Xian Li[1,3], Stefan Reinker[1], Robert M. Miura[1,4,5], and Richard S. Neuman[6]

[1] Department of Mathematics and
Institute of Mathematical Sciences
University of British Columbia, Vancouver, BC Canada V6T 1Z2

[2] Harvard-MIT Division of Health Sciences and Technology
Cambridge, MA 02139 USA

[3] Department of Zoology, University of British Columbia
Vancouver, BC Canada V6T 1Z2

[4] Department of Pharmacology and Therapeutics
University of British Columbia, Vancouver, BC Canada V6T 1Z3

[5] Departments of Mathematical Sciences and
Biomedical Engineering and
Center for Applied Mathematics and Statistics
New Jersey Institute of Technology, Newark, NJ 07102 USA

[5] Faculty of Medicine, Memorial University
St. John's, Newfoundland, Canada A1B 3V6

CAMS Report 0203-22, Spring 2003

Center for Applied Mathematics and Statistics

NJIT

The Influences of I_h on Temporal Summation in Hippocampal CA1 Pyramidal Neurons: A Modeling Study

ADRIEN E. DESJARDINS[1], YUE-XIAN LI[1], STEFAN REINKER[1,2], ROBERT M. MIURA[1,2,3], RICHARD S. NEUMAN[4]

Departments of Mathematics[1] and Pharmacology & Therapeutics[2], University of British Columbia, Vancouver, British Columbia, Canada

Department of Mathematical Sciences[3], New Jersey Institute of Technology, Newark, New Jersey, USA

Faculty of Medicine[4], Memorial University, St. John's, Newfoundland, Canada

Address for correspondence:

Richard S. Neuman
Faculty of Medicine
Memorial University
St. John's, Newfoundland
Canada, A1B 3V6
Phone: (709) 777-6887
Fax: (709) 777-7010
E-mail: rneuman@mun.ca

Abstract

Recent experimental and theoretical studies have found that active dendritic ionic currents can compensate for the effects of electrotonic attenuation. In particular, temporal summation, the percentage increase in peak somatic voltage responses invoked by a synaptic input train, is independent of location of the synaptic input in hippocampal CA1 pyramidal neurons under normal conditions. This independence, known as normalization of temporal summation, is destroyed when the hyperpolarization-activated current, I_h, is blocked [Magee JC (1999), *Nature Neurosci.* 2:508-514]. Using a compartmental model derived from morphological recordings of hippocampal CA1 pyramidal neurons, we examined the hypothesis that I_h was primarily responsible for normalization of temporal summation. We concluded that this hypothesis was incomplete. With a model that included I_h, the persistent Na^+ current (I_{NaP}), and the transient A-type K^+ current (I_A), however, we observed normalization of temporal summation across a wide range of synaptic input frequencies, in keeping with experimental observations.

Keywords

I_h, I_{NaP}, I_A, temporal summation, normalization, synaptic integration, compartmental modeling

Introduction

Pyramidal neurons found in the mammalian cerebral cortex and hippocampus have long apical dendrites that integrate input from the large number of excitatory and inhibitory synapses found on their surfaces. Passive cable theory predicts that somatic excitatory post-synaptic potentials (EPSPs) invoked by synaptic input vary in shape and amplitude according to the location of synaptic input (reviewed by Segev and London, 1999, 2000). EPSPs arising from synaptic inputs at distal dendritic locations are broader than those arising from synaptic inputs at locations more proximal to the soma, and therefore they summate more efficiently. Temporal summation, defined as the percent increase in peak somatic voltage responses invoked by a train of synaptic inputs, quantifies the extent to which EPSPs can summate to produce a larger response. Within the context of passive cable theory, therefore, temporal summation is dependent on the location of synaptic input. The dependence of temporal summation on the location of synaptic input may have significant implications for the processing of such input (see Cook and Johnston, 1999).

A growing body of experimental evidence has made it clear that active ion channels play an important role in determining the shape and the amplitude of EPSPs (reviewed in Johnston et al., 1996; Magee, 1999b; Segev and London, 2000; Yuste and Tank, 1996). In addition to ligand gated channels, a variety of voltage gated Na^+, K^+, Ca^{2+}, and Na^+/K^+ ion channels are found on dendrites (Magee, 1999b). These channels are subject to modulation by second messengers (Magee, 1999b), suggesting that synaptic integration is dynamic, non-uniform along the dendrite, and changes with the

behavioral state of the organism (Migliore et al., 1999; Schwindt and Crill, 1997; Segev and London, 2000). Moreover, some voltage-dependent currents that might be involved in the dynamics of synaptic integration, such as the hyperpolarization activated current (I_h), exhibit non-uniform distributions of maximum conductance per unit area along the soma-dendritic axis (reviewed by Magee, 1999b).

Recent experimental and theoretical studies have found that voltage-dependent ion channels can compensate for the effects of electrotonic attenuation in dendrites (Williams and Stuart, 2000; Berger et. al., 2001; Cook and Johnston, 1999). In the case of hippocampal CA1 pyramidal neurons, the magnitude of temporal summation arising from synaptic inputs on the soma is identical to that from synaptic inputs on the lower apical dendrite (the soma and dendritic region up to 350 μm from the soma), a condition called normalization of temporal summation (Magee, 1999a). While temporal summation increases with the frequency of synaptic input, normalization is observed over a wide range of frequencies. An example of normalization of temporal summation for a 50 Hz input at 350 μm from the soma is shown in Fig. 1. When I_h is blocked pharmacologically, normalization of temporal summation is lost (Fig. 1) (Magee, 1999a). It has been hypothesized that the kinetic properties of I_h (see Pape, 1996, for review) and the spatial gradient of I_h (Magee, 1998) are the primary factors needed to achieve normalization of temporal summation (Magee, 1999a).

The purpose of this study was to model the influences of I_h on temporal summation in hippocampal CA1 pyramidal neurons. Using a compartmental model derived from morphological recordings, we sought to reproduce the conditions leading to

normalization of temporal summation with physiologically plausible gradients of the maximum conductances per unit area for the passive leak current (I_{leak}) and for I_h. We also considered the effects of the persistent sodium current (I_{NaP}) and the transient A-type potassium current (I_A) on temporal summation (Williams and Stuart, 2000).

Methods

Morphological data for a rat CA1 hippocampal neuron collected from *in vivo* measurements (Buzsaki and Turner, 1998) were obtained from the Duke-Southampton archive of neuronal morphology (Cannon *et al.*, 1998b). The reconstructed neuron (neuron "n408" in the archive) is shown in Fig. 2A. All simulations were carried out using NEURON, Version 5.2 (Hines and Carnevale, 1997), and conversion of the morphological data to a form readable by NEURON was performed with cvapp (Cannon, 1998a). Matlab (Mathworks, Inc., 1998) was employed for additional data analysis. The NEURON codes used in this paper are available from the authors upon request.

Simulations were performed on a neuron, excluding the axon, modeled as a set of interacting compartments (*segments* in NEURON terminology). In order to compute time-varying membrane voltages, the axial currents and membrane currents were determined by using the voltage differences between adjacent compartments, and membrane currents were represented by their values in each compartment (Hines and Carnevale, 1997). The resulting ordinary differential equations (ODEs) for the voltages, one for each compartment, were conservation of current statements in Hodgkin-Huxley form. The ODE for a particular compartment assumed the form:

$$(1) \qquad C_m \frac{dV}{dt} + \sum_j I_j(V) = I_{app} - \sum_n \frac{V - V_n}{R_A}$$

where V is the voltage of the compartment, C_m is the compartmental membrane capacitance, $I_j(V)$ is the j^{th} ionic membrane current, I_{app} is the applied current (this was present in only one compartment), V_n is the voltage of the n^{th} adjacent compartment, and R_A is the axial resistance between the centers of adjacent compartments. In all compartments, the specific intracellular resistivity that determined R_A was 100 Ω cm and the capacitance per unit area was 1 μF/cm^2.

We considered combinations of four ionic currents in our model: the passive leak current (I_{leak}), the hyperpolarization-activated current (I_h), the persistent sodium current (I_{NaP}), and the transient A-type potassium current (I_A). These combinations and their consequences are described in the Results section. In the model containing only I_{leak} and I_h, the input impedances, time constants, and resting membrane potentials were consistent with corresponding data from hippocampal CA1 pyramidal neurons (Magee, 1998). Ionic membrane currents were modeled with the Hodgkin-Huxley formalism.

The model for I_{leak} was:

$$I_{leak} = \frac{V - V_{leak}}{R_m} \tag{2}$$

where in all compartments V_{leak} = -65 mV and R_m = 33.2 kΩ cm^2.

The model for I_h, obtained from Huguenard and McCormick (1992), was:

$$I_h = g_h\, h\, (V - V_h),$$

$$\frac{dh}{dt} = \frac{h_\infty - h}{\tau},$$

$$h_\infty = \frac{1}{1 + \exp\left(\frac{V + 75}{5.5}\right)},$$

(3) $$\tau = \frac{1}{\exp(-0.086V + 14.6) + \exp(0.07V - 1.87)},$$

where V_h = - 43 mV. The maximum conductance per unit area, g_h, was varied spatially. It increased linearly from 0.1 mS/cm^2 in the soma and basal dendrites to 0.7 mS/cm^2 at 350 μm from the soma on the apical dendrite. In the upper apical dendrites, farther than 350 μm from the soma, it was fixed at 0.7 mS/cm^2. The values at the soma and at 350 μm on the apical dendrite were consistent with observations of hippocampal CA1 pyramidal neurons (Magee, 1998), although the linearity of the increase and the constancy at other locations were simplifications.

The persistent sodium current was modeled by:

$$I_{NaP} = g_{NaP}\, m_\infty\, (V - V_{NaP}),$$

(4) $$m_\infty = \frac{1}{1 + \exp\left(\frac{-(V + 49)}{5}\right)}.$$

This model was based on the I_{NaP} model of Lipowsky et al. (1996). The activation variable m was always taken to be its steady-state value to reflect the faster gating of I_{NaP} with respect to that of I_h. The spatial gradient of g_{NaP} was chosen as described in the Results section.

The transient A-type potassium current was modeled by:

(5) $$I_A = g_A m^4 h (V - E_K)$$

where E_K = -80 mV. This model was presented in Hoffman et al. (1997). The kinetics for both m and h are different for channels within 100 μm of the soma than for those at a

greater distance. The maximum conductance density, as parameterized by g_A, had the following linear spatial distribution

(6) $$g_A = f_A\left(0.007 + 0.011 * \left[\text{distance from the soma in } \mu\text{m} / 100\right]\right)$$

in the regions of the apical dendrites that were within 100 μm of the soma. It was constant in other regions of the model neuron, assuming the value $0.018 f_A$ in regions of the apical dendrites that were farther than 100 μm from the soma, and the value $0.007 f_A$ in the basal dendrites. The scale factor f_A, which was identical at all locations in the model neuron, represents a departure from the model of Hoffman et al. (1997) and was chosen as described in the Results section.

Synaptic inputs were modeled as ideal current sources (Cook and Johnston, 1999). Each input consisted of a train of 5 dual-exponential current pulses (Fig 2B) to simulate excitatory postsynaptic currents (EPSCs) of the form:

(7) $$I_{\text{syn}} = A \exp(-t/\tau_{off}) [1 - \exp(-t/\tau_{on})], \qquad 0 \le t \le 1/f,$$

where A = 0.1 nA, τ_{on} = 0.4 ms, τ_{off} = 5 ms (Magee, 1999a), and f is the frequency of the synaptic input. Responses to synaptic inputs at frequencies between 20 Hz and 100 Hz were examined. Simulated synaptic inputs were applied only in the lower apical dendrite.

Hippocampal CA1 neurons contain dendritic spines that affect their electrotonic properties. To incorporate dendritic spines into our model, we adjusted R_m and C_m as described by Holmes and Rall (1992) and Rapp et al. (1992):

(8) $$R'_m = \frac{R_m}{F}, \; C'_m = C_m F$$

where $F = (\text{dendrite area} + \text{spine area})/\text{dendrite area}$. We chose a linear density of 3 spines per μm and an area of 1.25 μm^2 per spine, which is consistent with experimental measurements (Koch, 1999).

As recommended by De Schutter and Bower (1994), all compartment lengths were less than or equal to 0.05λ where λ is the compartmental electrotonic length calculated from the local passive membrane parameters. Compartment lengths in the lower apical dendrite were less than or equal to 0.005λ. The latter requirement was chosen subjectively by examining the convergence of voltage-time curves with respect to the lengths of compartments in the lower apical dendrite. The backward Euler method with a temporal step size of 0.5 ms was used for numerical integration.

We define temporal summation as [(EPSP5 – EPSP1)/EPSP1] × 100 (see Magee, 1999a) where EPSP1 and EPSP5 are the amplitudes of the first and fifth voltage responses that are evoked by a train of synaptic inputs (Fig. 2B). In those cases where a distinct maximum corresponding to the magnitude of EPSP1 was not apparent in the summation, EPSP1 was defined as the amplitude of the response evoked by a single synaptic input.

Results

In the passive model, the equations governing membrane potential were linear; therefore, the somatic voltage response to a train of synaptic inputs can be considered as the superposition of voltage responses from individual synaptic inputs. Since somatic voltage responses are broader for distal synaptic inputs than for proximal synaptic inputs,

temporal summation is an increasing function of the distance between the synaptic input and the soma (Segev and London, 1999). When the frequency of synaptic input is very low, i.e., excitatory post-synaptic currents (EPSCs) are widely separated in time, temporal summation does not take place since the voltage response resulting from a particular EPSC is effectively zero at the onset of the voltage response from the following EPSC. As the frequency of synaptic input increases, temporal summation grows, approaching the theoretical maximum of 400 percent for a linear system, in which case the onset of each voltage response coincides with the maximum value of the previous voltage response. For all intermediate cases, temporal summation is an increasing function of stimulus frequency.

When I_h was added to the passive model, temporal summation of somatic EPSPs was reduced for synaptic input at all locations on the lower apical dendrite. This is illustrated for the particular cases of somatic and distal synaptic input in Fig. 2B, where voltage responses to somatic and distal current injections are contrasted with corresponding voltage responses from the passive model. In the presence of I_h, the equations for membrane potential are no longer linear, so a somatic voltage response to a train of EPSCs is no longer a superposition of voltage responses to individual EPSCs. The reduction in temporal summation can be explained by the following argument: as I_h is voltage-dependent, it deactivates when the membrane is depolarized by synaptic input. The time constant for I_h is longer than the period of the synaptic inputs, so I_h is more deactivated during the later EPSPs. As I_h deactivates and its depolarizing influence is reduced, the membrane potential hyperpolarizes (Magee, 1999a). The result is that EPSPs evoked later in time are reduced in amplitude to a greater extent than those evoked earlier

in time. At high frequencies, deactivation of I_h is less significant than the broadening of voltage responses, and consequently distal synaptic inputs yield larger temporal summation than do proximal synaptic inputs. For lower frequencies, I_h deactivation is more significant. Distal synaptic inputs yielded slightly smaller temporal summation than did somatic synaptic inputs for $f < 27$ Hz (Fig. 3).

For frequencies near 27 Hz, the model with only I_{leak} and I_h yielded approximately equal temporal summation for distal and proximal inputs (Fig. 3), as well as for synaptic inputs at intermediate locations (data not shown). While we observed normalization in a narrow frequency range, Magee (1999a) observed normalization for a wide range of frequencies (Fig 4). Factors that might account for this discrepancy include: 1) I_{leak} and I_h were sufficient by themselves to yield normalization of temporal summation across a broad range of frequencies, but the spatial gradients of I_{leak} and I_h were inappropriate; 2) the kinetic parameters of our I_h model were inappropriate; and 3) an additional current was influential in determining the frequency sensitivity of temporal summation.

Our simulations suggest that I_{leak} and I_h alone were not solely responsible for normalization of temporal summation over the 20-50 Hz synaptic input frequency range. To test this, we considered different spatial gradients of I_{leak} and I_h. These distributions, which represent a temporary departure from those described in the Methods section, assumed the form:

$$\bar{g}_j(x) = \begin{cases} a_j + b_j x & \text{lower apical dendrites } (0 \le x \le 350) \\ a_j + 350 b_j & \text{upper apical dendrites } (x > 350) \\ a_j & \text{soma and basal dendrites} \end{cases} \tag{9}$$

where x is the distance from a point on the apical dendrites to the soma in μm and the subscript j specifies the current. The kinetics of I_h were those of the base model (Methods). We varied the parameters a_{leak} and a_h independently between values 10 times smaller and larger than the respective maximum somatic conductance of our base model (Methods), in logarithmic increments. For each pair of values (a_{leak}, a_h), we varied the values (b_{leak}, b_h) independently between those that produced 10-fold decreases in maximum conductance along the apical dendrite and those that produced 10-fold increases. We imposed two criteria on these distributions: *i*) normalization of temporal summation to within five percent for frequencies between 20 and 50 Hz; and *ii*) positive temporal summation for synaptic input from all locations and frequencies. While most distributions yielded temporal summation for a small range of stimulus frequencies, none of the distributions satisfied both criteria. As a representative example, we discuss the case where $g_{leak}(x)$ assumed the value of the base model, $(33.2\ \text{k}\Omega\ \text{cm}^2)^{-1}$, and $g_h(x)$ was of the form $g_h(x) = a + bx$ where $a = g(0)$ and $b = 6a/350$, resulting in a seven-fold increase in g_h along the lower apical dendrite (Fig. 5A). The difference between temporal summation from distal and somatic EPSPs decreased with increasing density of I_h channels (Fig. 5B). When g_h was small, this difference was large and positive for frequencies of both 20 Hz and 50 Hz, and temporal summation was positive. When g_h was large, the difference was small and negative, but temporal summation was also negative so that both *i*) and *ii*) were not satisfied.

To determine whether altering the kinetic parameters of our I_h model would result in normalization of temporal summation at all frequencies between 20 and 50 Hz, we

considered shifts in the voltage dependencies of h_∞ and τ that were parameterized by δ_1 and δ_2, respectively, so that (3) becomes:

$$h_\infty = 1/[1 + \exp((V + \delta_1 + 75)/5.5)],$$

$$\tau = 1/[\exp(-0.086(V + \delta_2) + 14.6) + \exp(0.07V - 1.87)]. \quad (10)$$

We varied δ_1 and δ_2 independently between -10 mV and 10 mV. These variations were combined with the fixed spatial distribution of I_{leak} channel density specified in our base model (Methods). Neither of the criteria, *i*) nor *ii*), were satisfied in any of these cases. In the remainder of this section, the spatial distributions of I_h and I_{leak} channels are those described in the Methods section.

Evidence for the influence of another current besides I_h and I_{leak} on temporal summation can be found in Magee (1999a), in which it was observed that the fifth EPSP evoked from distal sites was more than 400% larger than the first EPSP when I_h was blocked with ZD7288 (Fig 4). This result is inconsistent with a passive model, in which an increase in excess of 400% is not possible. A plausible candidate for the "missing" current is I_{NaP}, which is present in CA1 neurons and is capable of boosting EPSPs (Lipowsky et al., 1996). To test this hypothesis, we employed the spatial gradients of I_h and I_{leak} of our base model (Methods) and varied the spatial gradient of I_{NaP} using the functional form (9). We found that for the linear distribution determined by g_{NaP}(0 μm) = 0.27 mS/cm^2 at the soma and g_{NaP}(350 μm) = 1.3 mS/cm^2, normalization of temporal summation was independent of stimulus frequency for the range of 20 to 60 Hz (Fig. 6A). As expected, the addition of I_{NaP} increased the magnitude of temporal summation. Removal of I_h from the model destroyed the normalization. Despite displaying normalization of temporal summation that was dependent on the presence of I_h, the model

with only three currents, I_{leak}, I_h, and I_{NaP} displayed characteristics not in keeping with observation: the resting potentials for the compartments were in the vicinity of -43 mV, which is too depolarized, and the falling phase of the EPSP was prolonged as compared with experimental observations. These characteristics were eliminated following the incorporation of I_A into the model.

To create the model that included I_A, we once again assumed that the I_{NaP} channels had a spatial density of the functional form (9), and we assumed that the density of I_A channels, as parameterized by g_A, was identical at all locations in the model neuron. The maximum conductances per unit area for the currents I_{leak} and I_h were unchanged. For the distributions described by $g_{NaP}(0\ \mu m) = 1.07\ mS/cm^2$, $g_{NaP}(350\ \mu m) = 8.77\ mS/cm^2$, and $g_A = 0.35\ mS/cm^2$, normalization of temporal summation was independent of stimulus frequency for the range of 20 to 90 Hz (Fig. 6B). We found a wide range of distributions that yielded normalization of temporal summation, but the magnitude of temporal summation for a stimulation frequency of 50 Hz was close to that observed experimentally (Fig 4) for only the distribution above. Normalization was destroyed when I_h was removed from this model (Figs. 6B, 7). Resting potentials were in the vicinity of -57 mV, and the overall shapes of the EPSPs (Fig. 8) were consistent with experimental observations (Fig. 1). Moreover, the magnitude of temporal summation was reduced. The value of g_A is smaller than the one considered in the model by Hoffman et al. (1997). This difference may reflect the absence of other types of ionic currents in our model. Differences in temporal summation from stimulation at somatic and distal locations were relatively insensitive to small changes in the spatial distributions of I_A and I_{NaP} maximum conductances (Fig. 9). This suggests that normalization of temporal

summation is not dependent on very sharp tuning of ionic current distributions, although this situation might change on further addition of currents not present in the model.

In keeping with observation, local temporal summation, the percentage increase in voltage response at the location of synaptic input along the primary apical dendrite, decreased with distance from the soma in the range of 125 to 350 μm (Fig. 10). The magnitude of local temporal summation was dependent on the presence of I_h, I_{NaP}, and I_A. Local summation was highest when only I_{NaP} and I_A were present and lowest in the passive case, while the intermediate case was obtained when I_h, I_{NaP}, and I_A were present (Fig. 10). The magnitudes of the decreases (passive model: 45% decrease; I_{leak}, I_{NaP}, and I_A: 39%; I_{leak}, I_h, I_{NaP}, and I_A: 46%) were similar to those observed experimentally.

The magnitude of temporal summation decreased with increasing stimulus intensity. Temporal summation decreased from 95% to 47% for distal inputs of 50 Hz with peak EPSC amplitudes of 0.038 and 0.15 nA, respectively; the relationship between temporal summation and stimulus intensity was approximately linear for intermediate EPSC amplitudes. Despite this stimulus dependence, normalization of temporal summation occurred for all inputs in this range, for synaptic input frequencies between 20 to 90 Hz.

To determine whether the model with I_{leak}, I_h, I_{NaP}, and I_A would yield similar results with a different dendritic morphology, we applied it to a second reconstructed hippocampal CA1 neuron from the Duke-Southampton archive of neuronal morphology (neuron "n423" in the archive; see Fig. 11A). For this neuron, we obtained normalization of temporal summation at frequencies of 20 to 60 Hz (Fig. 11B), with summation at 50

Hz close to the observed value of 80%, by varying the distributions of I_A and I_{NaP} conductances as described above for the first neuron. The distributions obtained were similar to those of the first neuron considered (g_{NaP}(0 μm) = 1.49 mS/cm^2, g_{NaP}(350 μm) = 7.3 mS/cm^2, and g_A = 0.61 mS/cm^2). The ratio of g_{NaP}(0) to g_{NaP}(350 μm) was 4.8 for both neurons.

Discussion

Our principal finding is that normalization of temporal summation in hippocampal CA1 pyramidal neurons (Magee, 1999a) can be replicated by a realistic compartmental model employing a combination of I_{leak}, I_h, I_{NaP}, and I_A. In our model, temporal summation was independent of the location of synaptic input for frequencies between 20 Hz and 90 Hz in one neuron and 20 Hz to 60 Hz in the other, and assumed magnitudes comparable to those observed experimentally. In the absence of I_h, temporal summation was strongly dependent on both the frequency and the location of synaptic input, as observed experimentally (Figs. 1, 4) (Magee, 1999a).

Modeling reveals that EPSPs evoked on distal dendrites results in greater temporal summation at the soma than EPSPs evoked directly at the soma. EPSPs arriving from distal dendrites undergo significant low pass filtering by the dendritic capacitance, broadening these EPSPs compared to those evoked at the soma (Segev and London, 1999). The longer falling phase of distal EPSPs allows for greater summation at the soma for stimulation frequencies in which the rising phase of an EPSP overlaps that of the falling phase of the preceding EPSP. When I_h is present, the length of the decay phase of the EPSP is decreased. As the membrane is depolarized by a simulated EPSC, the resting inward current induced by I_h is inactivated, effectively decreasing the length

of the falling phase of the EPSP. Since the density of I_h channels increases with distance from the soma, local temporal summation in the dendrite is smaller than local summation at the soma (Fig. 10). The decrease of I_h along the dendrite shortens the falling phase of the EPSP, exactly counteracting the broadening effect of the dendritic capacitance. The non-uniform distribution of I_h ensures that EPSPs evoked proximal to the soma experience less decay than those evoked at distal sites. Despite the slower rising phase of the EPSPs that originate from the distal dendritic inputs, illustrating the expected capacitance induced broadening, the falling phase decays at a rate similar to that of the somatically evoked EPSP (Fig. 12). Consequently, the magnitude of the temporal summation is normalized. At high stimulation frequencies, the slow time constant of I_h inactivation is not sufficient to generate sufficient decay of the EPSP to match the filtering action of dendritic capacitance and normalization fails.

Our compartmental model of both pyramidal neurons included extensive branching in the basal and upper apical dendrites. In preliminary simulations, a model in which the basal and upper apical dendrites were absent and closed-end boundary conditions were employed produced significantly different results than our full model, particularly with respect to local temporal summation. Explicit inclusion of the apical and basal dendrites reduced the uncertainties that would have been involved in creating an equivalent dendrite, with the tradeoff of introducing additional model parameters.

The distributions of I_{leak} and I_h in the lower apical dendrite employed in our model are in agreement with whole cell recordings from CA1 neurons (Magee, 1998). However, very little is known about the distributions of these ion channels in the basal

dendrites and upper apical dendrites. The assumption of constant channel densities in these regions may be inaccurate and could account for some of the differences between our modeling results and the experimental observations of Magee (1999a).

Our knowledge of the distribution of I_{NaP} in CA1 neurons is even less complete than for I_{leak} and I_h (Andreasen and Lambert, 1999; French et al., 1990; Lipowsky et al., 1996). Dendritic recordings reveal that the transient Na^+ channels (I_{Na}) are uniformly distributed along the lower apical dendrite (see Magee, 1999b). However, the much smaller I_{NaP} is thought to have the highest density of channels in the vicinity of the soma and a lower density in the dendrites (French et al., 1990). In our simulations, the distribution of I_{NaP} channels was chosen such that its addition to the model with I_{leak} and I_h resulted in normalization of temporal summation for synaptic input frequencies of 20 to 60/90 Hz and temporal summation of 80% for a stimulus frequency of 50 Hz. This constraint necessitated a 4.8 fold increase in I_{NaP} from the soma to 350 μm on the apical dendrite. The apparent discrepancy in the distribution of I_{NaP} required by our model on the one hand and that proposed by French et al. (1990) and modeled by Lipowsky et al. (1996) on the other, further highlights the question of the role of I_{NaP} in the normalization of temporal summation and the completeness of our model.

Normalization of temporal summation in CA1 and neocortical neurons is lost following the pharmacological blockade of I_h (Figs 1, 4) (Magee, 1999a; Williams and Stuart, 2000). From these experimental observations, however, it remains unclear which currents besides I_{leak} and I_h significantly affect temporal summation. We extensively tested models containing only I_{leak} and I_h, where each model contained a different

combination of I_h kinetics and spatial distributions of I_h and I_{leak} channel densities. From our results, we conclude that location and frequency independent temporal summation probably could not be achieved with a model containing only these two currents. Moreover, the magnitudes of temporal summation in our simulations with I_{leak} and I_h were noticeably smaller than observed in whole cell recordings from CA1 neurons (compare Figs. 3 & 4) (Magee, 1999a). This suggests that at least one additional membrane current is needed in order to explain the experimental findings. The dendrites of CA1 neurons also contain a variety of potassium currents (Hoffman et al., 1997). The transient A-type potassium current, I_A, has previously been implicated in the elimination of location-dependent variability (Cook and Johnston, 1999). The persistent sodium current, I_{NaP}, has been shown to boost temporal summation in neocortical neurons (Williams and Stuart, 2000). The I_{NaP} channels are activated by EPSPs on CA1 dendrites (Magee and Johnston, 1995) and might account for the supralinear temporal summation observed in CA1 neurons during the pharmacological blockade of I_h (Magee, 1999a). Adding I_{Nap} to the combined I_{leak} and I_h model boosted the magnitude of temporal summation. As expected, the addition of I_A reduced the magnitude of temporal summation. More importantly, with the chosen distribution, normalization of temporal summation was achieved for synaptic input frequencies of 20 to 60-90 Hz, depending on the dendritic morphology, and proved to be strongly dependent on the presence of I_h. In agreement with experimental observations (Magee, 1999a), local temporal summation declined with distance from the soma (Fig. 10).

The inclusion of I_{NaP} also caused the magnitude of temporal summation to be dependent on stimulus intensity, a feature not observed with the combined I_{leak} and I_h

model or experimentally (Magee, 1999a). This stimulus dependence was observed in both the presence and absence of I_A. In our model, stimulus dependent summation results from the non-linear amplification and attenuation of the EPSPs by voltage-dependent ionic currents. Since the magnitude of I_{NaP} increases with voltage, smaller EPSPs are amplified to a smaller extent than larger EPSPs. This amplification increases non-linearly with voltage, so that the effect of I_{NaP} is an increase in temporal summation for larger stimulus inputs. Conversely, I_A decreases summation values by attenuating the peak amplitude of the EPSP and reducing the slow falling phase of the EPSP. This attenuation increases non-linearly with voltage, so that the effect of I_A is a decrease in temporal summation for larger stimulus inputs. I_h has an effect similar to I_A. The effects of I_A and I_h in this context outweigh those of $I_{NaP,}$ resulting in the observed relationship between temporal summation and magnitude of stimulus input in our model.

The models of I_{NaP} and I_A used in our computations may partly reflect the contributions of several different voltage-dependent currents present in the dendrites of CA1 neurons as well as the ion channel distributions in the basal and apical dendrites. Potassium currents in CA1 dendrites alter dendritic excitability (see Johnston et al., 2000) and mask the appearance of I_{NaP} (Andreasen and Lambert, 1999; French et al., 1990). Several Ca^{2+} currents are present in CA1 dendrites (see Magee, 1999b). In particular, the T-type Ca^{2+} current can be activated by dendritic EPSPs (Magee and Johnston, 1995). Explicit addition of one or more voltage-dependent currents to the model could bring the distributions of I_{NaP} and I_A more in line with experimental observations and eliminate the stimulus dependence of summation magnitude. Since our primary goal in this study was to determine whether the properties of I_h could account for normalization of temporal

summation, we did not attempt to model these additional currents, which would introduce more free parameters that have not been measured experimentally. Quantifying the consequences of these currents on temporal summation could form the basis for more extensive modeling studies.

References

Andreasen M., Lambert JD (1999) Somatic amplification of distally generated subthreshold EPSPs in rat hippocampal pyramidal neurons. *J. Physiol.* 519: 85-100.

Berger T, Larkum ME, Luscher HR (2001) High *I(h)* channel density in the distal apical dendrite of layer V pyramidal cells increases bidirectional attenuation of EPSPs. *J. Neurophysiol.* 85: 855-868.

Buzsaki G, Turner DA (1998) Dendritic properties of hippocampal CA1 pyramidal neurons in the rat: Intracellular staining in vivo and in vitro. *J. Comp. Neurol.* 391: 335-352.

Cannon RC (1998a) cvapp: neuronal morphology viewer, editor and file converter. URL: http://www.cns.soton.ac.uk/~jchad/cellArchive/cellArchive.html.

Cannon RC, Turner DA, Pyapali GK, Wheal HV (1998b) An on-line archive of reconstructed hippocampal neurons. *J. Neurosci. Methods* 84:49-54. URL: http://www.cns.soton.ac.uk/~jchad/cellArchive/cellArchive.html.

Cook EP, Johnston D (1999) Voltage-dependent properties of dendrites that eliminate location-dependent variability of synaptic input. *J. Neurophysiol.* 81:535-543.

De Schutter, E, Bower, JM (1994) An Active Membrane Model of the Cerebellar Purkinje Cell I. Simulation of Current Clamps in Slice. *J. Neurophysiol*. 71:375-400.

French CR, Sah P, Buckett KJ, Gage PW (1990) A voltage-dependent persistent sodium current in mammalian hippocampal neurons. *J. Gen. Physiol.* 95:1139-1157.

Hines ML, Carnevale NT (1997) The NEURON simulation environment. *Neural Comput.* 9:1179-1209.

Hoffman DA, Magee JC, Colbert CM, Johnston D (1997) K^+ channel regulation of signal propagation in dendrites of hippocampal pyramidal neurons. *Nature* 387:869-875.

Holmes WR, Rall W (1992) Electrotonic length estimates in neurons with dendritic tapering or somatic shunt. *J. Neurophysiol.* 68:1421-1437.

Huguenard JR, McCormick DA (1992) Simulation of the currents involved in rhythmic oscillations in thalamic relay neurons. *J. Neurophysiol.* 68:1373-1383.

Johnston D, Hoffman DA, Magee JC, Poolos NP, Watanabe S, Colbert CM, Migliore M (2000) Dendritic potassium channels in hippocampal pyramidal neurons. *J. Physiol.* 525(1): 75-81.

Johnston D, Magee JC, Colbert CM, Christie BR (1996) Active properties of neuronal dendrites. *Ann. Rev. Neurosci.* 19:165-186.

Koch, C (1999) Biophysics of Computation: Information Processing in Single Neurons. Oxford University Press, Oxford.

Lipowsky R, Gillessen T, Alzheimer C (1996) Dendritic Na^+ channels amplify EPSPs in hippocampal CA1 pyramidal cells. *J. Neurophysiol.* 76:2181-2191.

Magee JC (1998) Dendritic hyperpolarization-activated currents modify the integrative properties of hippocampal CA1 pyramidal neurons. *J. Neurosci.* 18:7613-7624.

Magee JC (1999a) Dendritic I_h normalizes temporal summation in hippocampal CA1 neurons. *Nature Neurosci.* 2:508-514.

Magee JC (1999b) Voltage-gated ion channels. In: Stuart G, Spruston N, Hausser M, eds. *Dendrites*. Oxford University Press, Oxford. pp. 139-160.

Magee JC, Johnston D (1995) Synaptic activation of voltage-gated channels in the dendrites of hippocampal pyramidal neurons. *Science* 268: 301-304.

Migliore M, Hoffman DA, Magee JC, Johnston (1999) Role of an A-type K+ conductance in the back-propagation of action potentials in the dendrites of hippocampal pyramidal neurons. *J Comput. Neurosci*. 7:5-15.

Pape H-C (1996) Queer current and pacemaker: The hyperpolarization-activated cation current in neurons. *Ann. Rev. Physiol.* 58:299-327.

Rapp M, Yarom Y, and Segev I (1992) The impact of parallel fiber background activity on the cable properties of cerebellar Purkinje cells. *Neural Comput.* 4:518-533.

Schwindt PC, Crill WE (1997) Modification of current transmitted from apical dendrite to soma by blockade of voltage- and Ca2+-dependent conductances in rat neocortical pyramidal neurons. *J. Neurophysiol.* 78:187-198.

Segev I, London M (1999) A theoretical view of passive and active dendrites. In: Stuart G, Spruston N, Hausser M, eds. *Dendrites*. Oxford University Press, Oxford. pp. 205-230.

Segev I, London M (2000) Untangling dendrites with quantitative models. *Science* 290: 744-750.

Williams SR, Stuart GJ (2000) Site independence of EPSP time course is mediated by dendritic I_h in neocortical pyramidal neurons. *J. Neurophysiol.* 83:3177-3182.

Yuste R, Tank DW (1996) Dendritic integration in mammalian neurons, a century after Cajal. *Neuron* 16:701-716.

Figure Legends

Figure 1. Normalization of temporal summation at CA1 neurons is dependent on the presence of I_h. Whole cell recordings from the soma of a CA1 neuron in vitro. EPSPs were simulated using exponential currents applied at a rate of 50 Hz to either the dendrite (through a second whole cell electrode) or the soma. Current magnitudes were adjusted to produce similar amplitudes of the first EPSP at the soma. Pharmacological blockade of I_h with 20 μM ZD7288 (lower records) eliminates normalization of temporal summation. Reproduced from Magee (1999a) with permission. © Nature Publishing Group.

Figure 2. Temporal summation in a model hippocampal CA1 pyramidal neuron is dependent on the location of synaptic input and the hyperpolarization activated current I_h. **A**. Morphology of the reconstructed neuron ("n408") used for the computer simulation. EPSCs were simulated at 0 μm (soma) and at 350 μm (distal) on the primary dendrite. **B**. Somatic voltage responses to distal and somatic EPSCs at 50 Hz. The dotted curves correspond to a passive model (only leakage conductance and capacitance were included). The solid curves reflect the addition of I_h to the model. For both distal and synaptic EPSCs, the addition of I_h resulted in a reduction of temporal summation.

Figure 3. Inclusion of I_h in a passive model provides normalization of temporal summation for a small range of EPSC frequencies. EPSCs were simulated separately at distal (triangles) and somatic (squares) locations on the apical dendrite with I_h absent (open symbols) and present (filled symbols). Temporal summation was normalized only at frequencies in a small range around 27 Hz (arrow). Temporal summation increased with frequency of synaptic input.

Figure 4. Normalization of temporal summation recorded in vitro from CA1 neurons is frequency independent over a wide range of frequencies, but shows clear failure by 100 Hz. Pharmacological blockade of I_h with 20 μM ZD7288 eliminates normalization. EPSP summation at the soma for exponential current injections at the soma (triangles) and distal dendrite at CA1 neurons in vitro with I_h present (open symbols) and I_h blocked by ZD7288 (filled symbols). Reproduced from Magee (1999a) with permission. © Nature Publishing Group.

Figure 5. When no other active currents are present, different spatial distributions of I_h conductances are required for normalization of temporal summation at 20 Hz and 50 Hz. **A.** The density of I_h conductances increased seven-fold on the primary apical dendrite from 0 μm (soma) to 350 μm (distal): $g_h(x) = g_h(0)[1 + 6x/350]$. **B.** The difference between temporal summation from distal and somatic EPSCs decreases with increasing density of I_h conductances. A necessary condition for normalization is that temporal summation from distal and somatic EPSCs are equal (dashed line). Different values of

$g_h(0)$ were required for normalization of temporal summation at 20 Hz (triangles) and at 50 Hz (circles).

Figure 6. A. Addition of the persistent Na^+ current (I_{NaP}) to the model neuron "n408" results in normalization of temporal summation of somatic and distal inputs for frequencies between 20 and 60 Hz. **B.** Addition of both the persistent Na^+ current (I_{NaP}) and the transient A-type potassium current (I_A) to the model neuron "n408" results in normalization of temporal summation of somatic and distal inputs for frequencies between 20 and 90 Hz. When I_h is absent (open symbols; both figures), distal EPSCs (triangles) yielded higher temporal summation than that from somatic EPSCs (squares). In the presence of I_h (filled symbols), distal and somatic EPSCs yielded identical summation. Summation values were generally lower when I_A was present than when it was absent, reflecting the hyperpolarizing effects of this current.

Figure 7. Temporal summation is independent of the location of synaptic input when I_{NaP}, I_A, and I_h are included in the model (filled triangles). When I_h was absent from the model (open triangles), temporal summation was dependent on the location of synaptic input. The EPSC frequency was 50 Hz. This result was characteristic of other EPSC frequencies in the range of 20 to 90 Hz.

Figure 8. EPSP amplitude is dependent on stimulus location and the presence of I_h. **A.** Somatic voltage responses to distal and somatic EPSCs at 50 Hz for the model with ionic currents I_{leak}, I_{NaP}, I_A, and I_h. EPSP amplitude is higher for somatic inputs than for distal inputs, but temporal summation is the same in both cases. **B.** Somatic voltage responses to distal and somatic EPSCs at 50 Hz for the model with ionic currents I_{leak}, I_{NaP}, and I_A (I_h absent). The voltages are higher than those from the corresponding voltages in A, which reflects the hyperpolarizing effects of I_h. Temporal summation was not equal for distal and somatic inputs in this case.

Figure 9. Differences between temporal summation from distal and somatic EPSPs were relatively insensitive to small changes in the spatial distributions of I_A and I_{NaP} conductances. The spatial distribution of I_{NaP} channels, as parameterized by g_{NaP}, was varied first by changing g_{NaP} uniformly for all compartments, from a 20% decrease to a 20% increase. Secondly, the spatial gradient of g_{NaP} was altered by changing the ratio of $g_{NaP}(350\ \mu m)$ to $g_{NaP}(0\ \mu m)$ ($g_{NaP}(350\ \mu m) \rightarrow g_{NaP}(350\ \mu m)\sqrt{k}$ and $g_{NaP}(0\ \mu m) \rightarrow g_{NaP}(0\ \mu m) / \sqrt{k}$, where k is the fractional change). Similarly, the magnitude of I_A channel density, as parameterized by g_A, was varied by changing g_A uniformly for all compartments. All three variations were performed independently of each other.

Figure 10. Local temporal summation along the primary apical dendrite varies with distance from the soma. Local temporal summation reflects the percentage increase in voltage response at the location of synaptic input. It was highest when both I_h and I_{NaP} were present (solid circles), and lowest when only I_{leak} was

present (solid squares). Temporal summation decreased with distance from the soma in the range of 150-350 μm, a result consistent with experimental observations (Magee, 1999a).

Figure 11. **A**. Morphology of the second reconstructed neuron ("n423") used for the computer simulation **B.** Frequency dependence of temporal summation of model neuron "n423" is similar to that of model neuron "n408" (see Fig. 4B). Addition of both the persistent Na^+ current (I_{NaP}) and the transient A-type potassium current (I_A) with similar maximum conductances per unit area as those in model neuron "n408" resulted in normalization of temporal summation of somatic and distal inputs for frequencies between 20 and 60 Hz.

Figure 12. Inactivation of I_h enhances the falling phase of EPSPs evoked at distal sites and matches the falling phase of EPSPs evoked at the soma, leading to normalization of temporal summation.

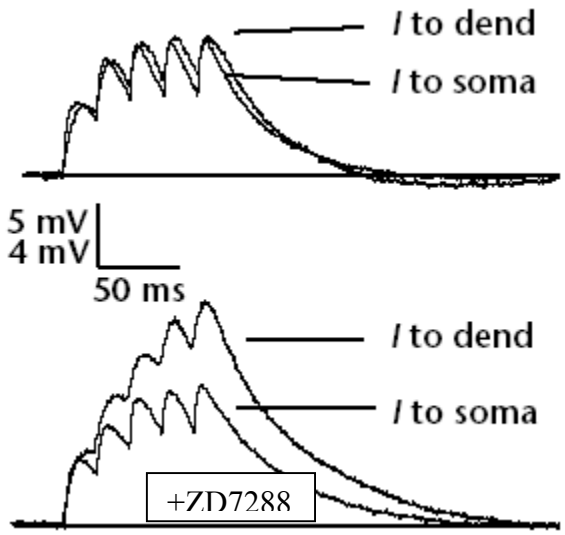

Fig 1

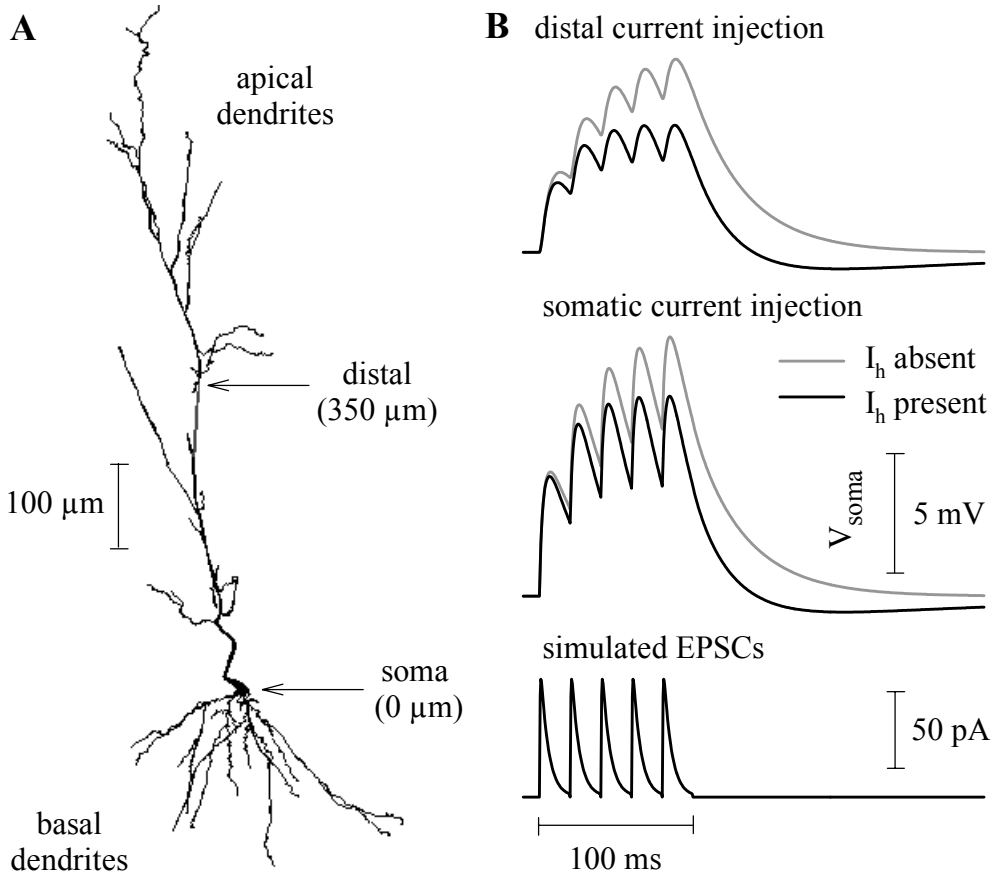
A
apical
dendrites
distal
(350 µm)
100 µm
soma
(0 µm)
basal
dendrites
B
distal current injection
somatic current injection
I_h absent
I_h present
V_soma
5 mV
simulated EPSCs
50 pA
100 ms

Fig 2

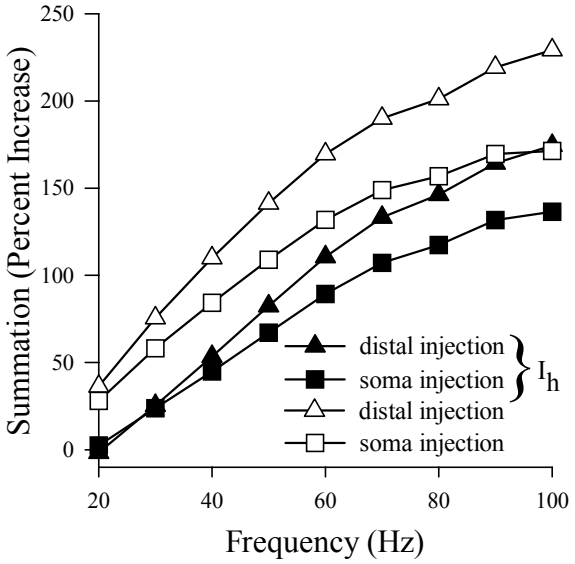
250
200
150
100
50
0
Summation (Percent Increase)
20
40
60
80
100
Frequency (Hz)
distal injection
soma injection
distal injection
soma injection
I_h

Fig 3

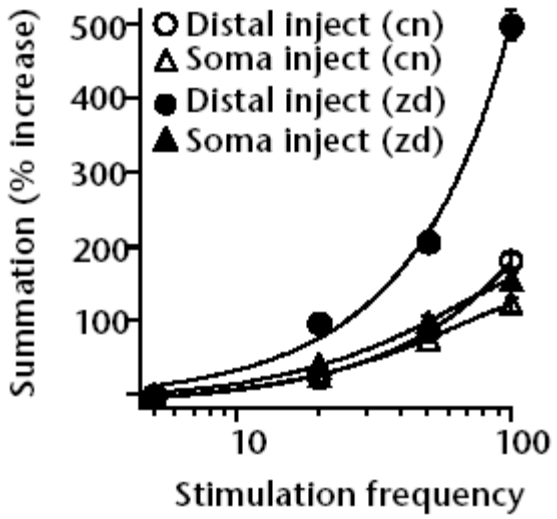
Summation (% increase)
500
400
300
200
100
Distal inject (cn)
Soma inject (cn)
Distal inject (zd)
Soma inject (zd)
10
100
Stimulation frequency

Fig 4

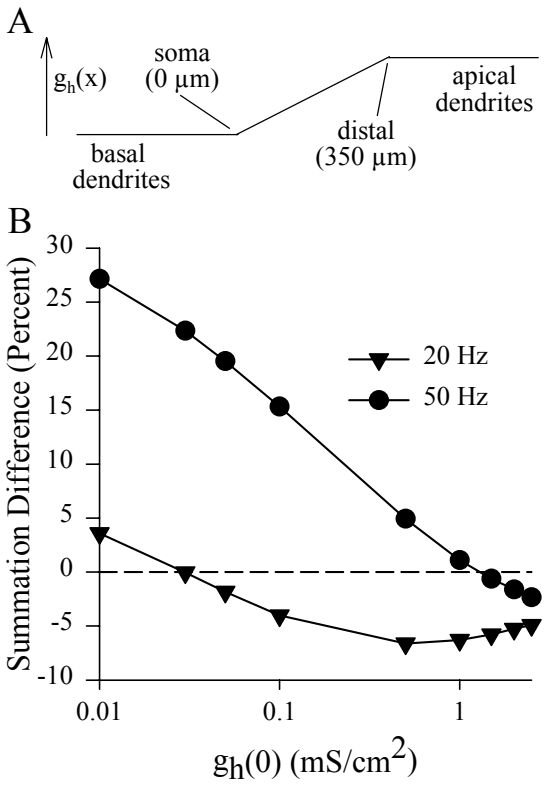
A
$g_h(x)$
soma
(0 µm)
apical
dendrites
distal
(350 µm)
basal
dendrites
B
Summation Difference (Percent)
30
25
20
15
10
5
0
-5
-10
0.01
0.1
1
20 Hz
50 Hz
$g_h(0)$ (mS/cm^2)

Fig 5

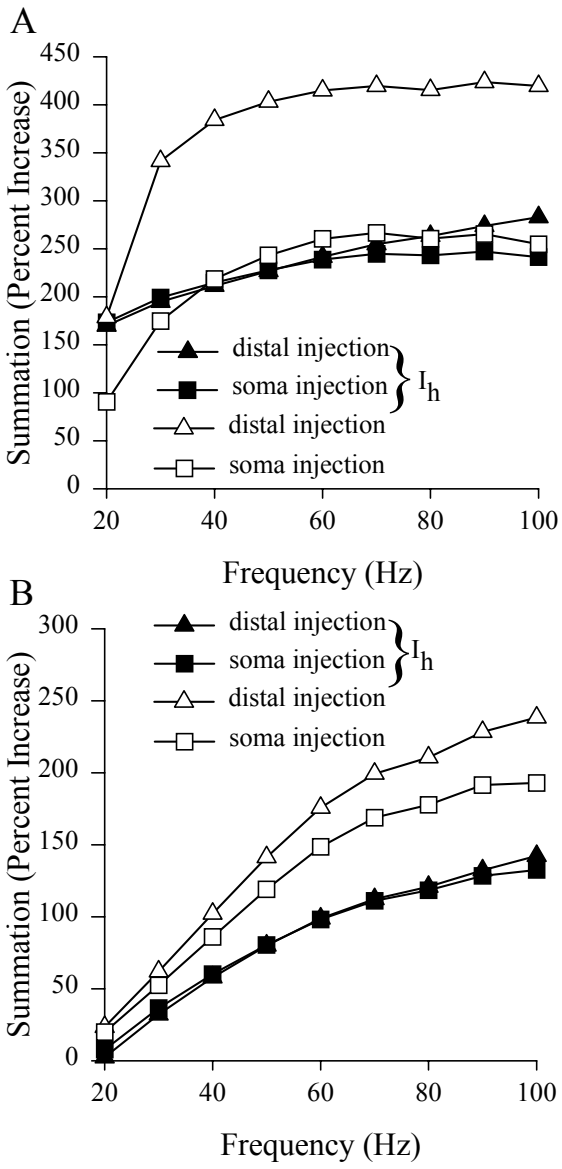
A
Summation (Percent Increase)
450
400
350
300
250
200
150
100
50
0
20
40
60
80
100
Frequency (Hz)
distal injection
soma injection
I_h
distal injection
soma injection
B
Summation (Percent Increase)
300
250
200
150
100
50
0
20
40
60
80
100
Frequency (Hz)
distal injection
soma injection
I_h
distal injection
soma injection

Fig 6

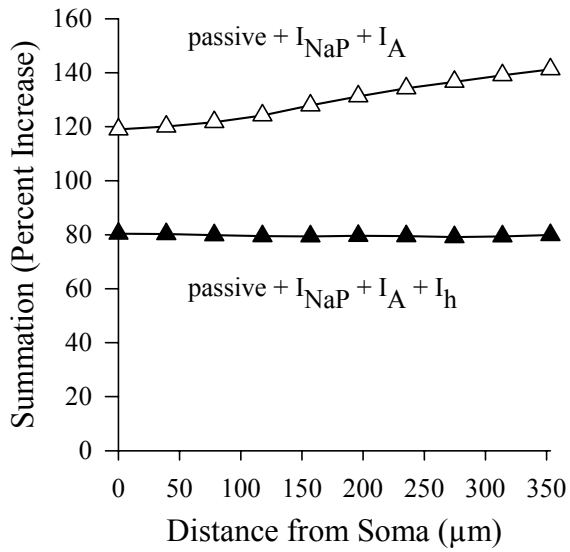
160
140
120
100
80
60
40
20
0
Summation (Percent Increase)
passive + I_{NaP} + I_A
passive + I_{NaP} + I_A + I_h
0
50
100
150
200
250
300
350
Distance from Soma (μm)

Fig 7

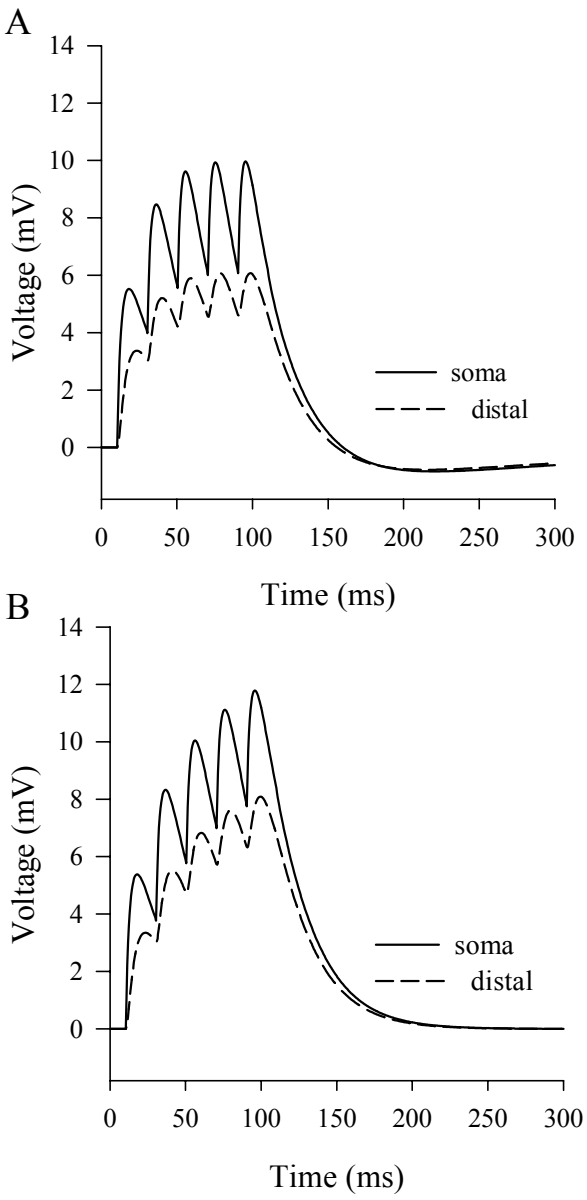
A
14
12
10
8
6
4
2
0
Voltage (mV)
soma
distal
0
50
100
150
200
250
300
Time (ms)
B
14
12
10
8
6
4
2
0
Voltage (mV)
soma
distal
0
50
100
150
200
250
300
Time (ms)

Fig 8

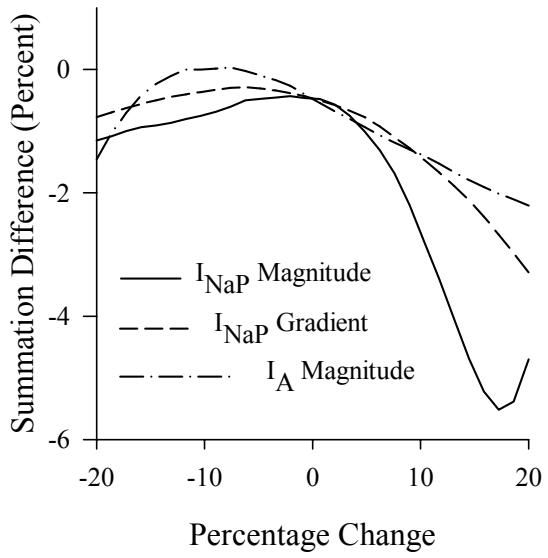
Summation Difference (Percent)
0
-2
-4
-6
-20
-10
0
10
20
Percentage Change
I_{NaP} Magnitude
I_{NaP} Gradient
I_A Magnitude

Fig 9

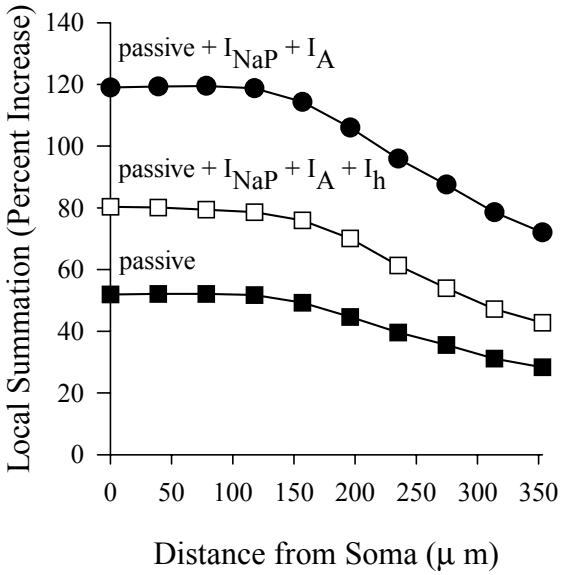
Local Summation (Percent Increase)
140
120
100
80
60
40
20
0
passive + I_{NaP} + I_A
passive + I_{NaP} + I_A + I_h
passive
0
50
100
150
200
250
300
350
Distance from Soma (μ m)

Fig 10

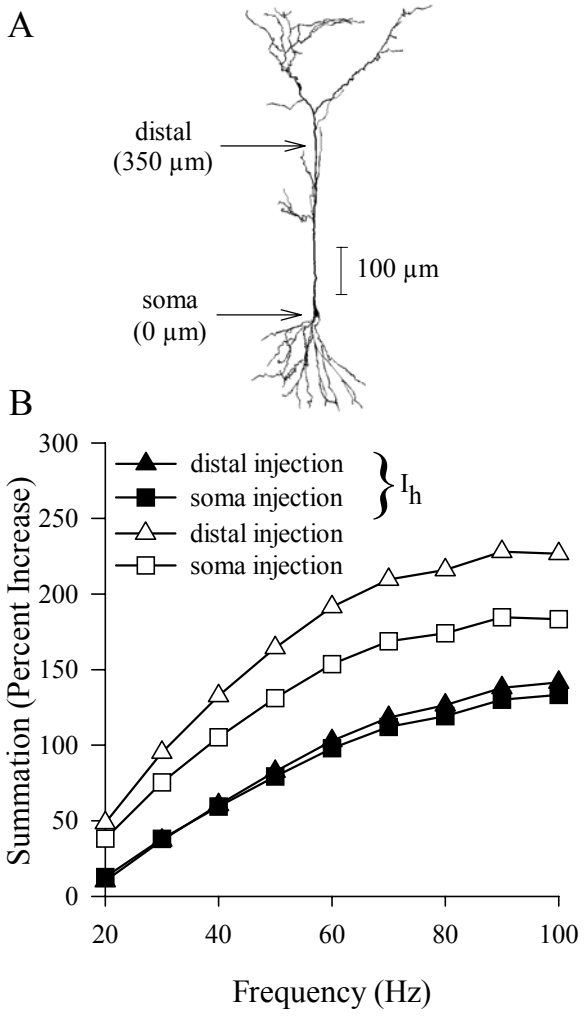
A
distal
(350 µm)
100 µm
soma
(0 µm)
B
300
250
200
150
100
50
0
Summation (Percent Increase)
distal injection
soma injection
distal injection
soma injection
Ih
20
40
60
80
100
Frequency (Hz)

Fig 11

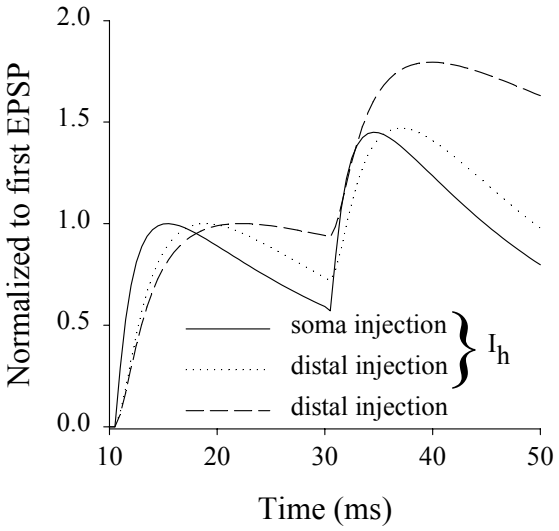
2.0
1.5
1.0
0.5
0.0
Normalized to first EPSP
soma injection
distal injection
distal injection
I_h
10
20
30
40
50
Time (ms)

Fig 12.